

中国激光

近红外二区荧光手术导航探针研究进展

韦族武, 杨森, 吴名, 刘小龙^{*}

福建医科大学孟超肝胆医院, 福建 福州 350025

摘要 肿瘤是严重威胁人类健康和社会发展的重大公共卫生问题之一。针对肿瘤的治疗, 外科手术切除仍是最普遍、最理想的策略。目前, 外科医师在术中主要通过肉眼观察、超声等方法确定肿瘤边界、残余病灶以及微小转移病灶, 然而, 这些方式存在手术切缘肿瘤易残留、难以实时发现微小转移灶等问题, 导致肿瘤术后复发、转移率高, 严重影响病人的预后和远期生存。荧光手术导航的快速发展为解决这一问题提供了新的技术支撑。本文聚焦于荧光手术导航用荧光探针, 重点对荧光手术导航系统和各类有机、无机近红外二区荧光分子探针进行系统阐述, 分析其临床转化与应用面临的瓶颈问题, 探讨可能的解决思路, 以期为国内外相关领域的研究提供思路与参考。

关键词 生物医学; 荧光手术导航; 荧光探针; 近红外二区; 腹腔镜手术系统; 分子影像探针

中图分类号 R454.2 文献标识码 A

DOI: 10.3788/CJL202249.0507102

1 引言

近年来, 肿瘤发病率在全球范围内呈高增长趋势。据统计, 2020 年全球新发肿瘤病人约 1930 万例, 死亡病人将近 1000 万例^[1]。目前, 手术仍是实体肿瘤治疗的首选方案。彻底切除肿瘤对于病人的预后和远期生存至关重要, 其中完全切除术后生存率可较部分切除术后生存率提高 2~5 倍。然而, 全球范围内肿瘤切除术后的平均复发率仍高达 40%, 导致其中约 80% 的病人死亡^[2-3]; 高术后复发率的主要原因是手术不彻底导致的肿瘤切缘残留、术中难以发现的微小转移灶或小病灶残留、淋巴结微转移等。在临床诊疗行为中, 医生在术前可借助超声成像、计算机 X 射线断层造影、正电子发射断层成像、核磁共振成像等影像手段进行精准的肿瘤定位和形态确认^[4]; 但在术中, 医生只能通过肉眼观察、触诊、超声检查等方法来确定肿瘤边界、病灶残余及微小转移灶, 检查手段非常有限, 易导致手术切缘残留或术中漏检微小病灶, 从而导致肿瘤术后的复发、转移率较高, 严重影响了病人的预后和远期生存。因此, 临幊上迫切需要发展一种无辐射、高灵敏度、高分辨率、高对比度、可在术中实时确定肿瘤边界并

显示重要管道结构以及发现微小转移病灶的技术手段, 以在术中实时引导手术的开展。在此背景下, 荧光手术导航技术应运而生。

荧光手术导航是指利用外源荧光分子探针的特异性标记肿瘤和重要的解剖结构, 在荧光成像系统的指引下, 在术中精准定位病灶并实时指引外科医生手术的过程。该技术不仅可以避免重要解剖结构的损伤, 还可以清晰地指示肿瘤边界, 帮助医生发现肿瘤切缘的少量残存肿瘤细胞以及术前影像难以发现的微小肿瘤病灶, 具有实时、高灵敏度、高分辨率、高对比度、无辐射等一系列优点, 目前已被广泛应用于前哨淋巴结的指示、肿瘤手术切除、重要神经和管道结构显示等临幊领域, 成为外科研究的前沿热点^[5]。荧光手术导航设备主要包括荧光手术导航系统和荧光分子影像探针两部分, 如图 1 所示。目前, 一系列近红外一区(NIR-I, 700~900 nm)荧光手术导航系统已经获批进入临幊, 该导航系统包括便携手持式系统、开放手术系统和腹腔镜手术系统^[6-9], 在乳腺癌^[10-11]、胃癌^[12-13]、肝癌^[14-15]、宫颈癌^[16]等肿瘤手术中被广泛应用。在临幊上使用的荧光分子探针主要包括荧光素钠^[17]、亚甲基蓝(MB)^[18-19]、5-氨基乙酰丙酸(5-ALA)^[20-21]、吲哚菁

收稿日期: 2021-12-01; 修回日期: 2021-12-24; 录用日期: 2022-01-14

基金项目: 国家自然科学基金(62175031, 61905043, 61727823)、福州市社会发展项目(2019-S-89)

通信作者: *xiaoloong.liu@gmail.com

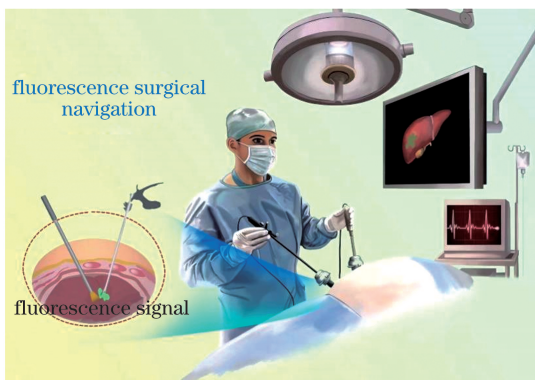


图 1 荧光手术导航技术

Fig. 1 Fluorescence surgical navigation technology

绿(ICG)^[22-24]等,其中 ICG 的应用最为广泛,已成为目前临幊上主要使用的荧光分子探针。然而,目前临幊上应用的 ICG 在 NIR-I 发光,且 ICG 本身无肿瘤特异靶向能力,存在穿透深度有限、背景信号强、信噪比欠佳、无肿瘤特异性、易产生假阳性等一系列问题。相比于 NIR-I 荧光,近红外二区(NIR-II, 1000~1700 nm)的荧光波长更长,能明显减少生物组织对光的吸收和散射,且能克服自体荧光的干扰,具有更深的组织穿透深度、更低的背景信号、更高的信噪比和空间分辨率^[25-26]。因此,NIR-II 荧光手术导航成为近年来手术导航领域的前沿研究热点,科研工作者围绕开发 NIR-II 手术导航系统、研制各类新型 NIR-II 荧光分子探针、增加荧光探针的

肿瘤靶向能力和靶向特异性等开展了系列工作。本文聚焦 NIR-II 荧光分子探针,围绕其手术导航应用,总结最新的研究进展,分析其临床转化面临的瓶颈问题,探讨可能的解决思路,为国内外相关领域的研究人员提供参考,以期推动 NIR-II 荧光手术导航技术的临床应用。

2 荧光手术导航系统

荧光手术导航技术依赖荧光成像系统和荧光探针在术中更精准地显示病灶信息。荧光手术导航系统的发展经历了手持式、开放式和内镜式三个发展阶段^[27],并且随着荧光分子探针的发展而发展。目前,已经有一系列荧光手术导航系统获批进入临幊应用或正在进行临幊试验,这些系统如表 1 所示^[27]。近年来,由于 ICG 探针在临幊上的广泛应用以及微创内镜技术的快速发展,再加上近红外光(700~900 nm)在组织中较低的吸收和散射特性,目前临幊上主流的荧光手术成像系统均已拓展到了 NIR-I,且整合到了腹腔镜等内镜系统中,代表性的产品包括加拿大 Novadaq 公司的 PINPOINT 系统^[28]、美国史赛克公司的 Stryker 1688AIM 4K^[29-31]和达芬奇机器人系统、中国科学院自动化研究所田捷教授团队创立的珠海市迪谱医疗科技有限公司的慧眼 H3000 系统^[32],以及广东欧谱曼迪科技有限公司的 Opto-4k 系列荧光导航内镜系统。

表 1 荧光手术导航系统^[27]
Table 1 Fluorescence surgical navigation system^[27]

Imaging system	Manufacturer	Main application	Excitation	Field of view	Resolution	Working distance / mm	Color video	Clinical status
SPY	Novadaq Technologies, Mississauga, Canada	Intraoperative fluorescence imaging	820 nm laser	190 mm×127 mm	Not specified	300	No	Food and Drug Administration (FDA) approved
Artemis	O2view, Marken, the Netherlands	Stereoscopic fluorescence imaging	400~1000 nm laser	22.5 mm×22.5 mm at 50 mm distance	659 pixel×494 pixel	≥50	Yes	FDA approved
Fluobeam	Fluoptics, Grenoble, France	Handheld fluorescence imaging	690 or 780 nm laser	128 mm×94 mm	640 pixel×480 pixel	150	No	Clinical trial
FLARE	Frangioni Laboratory, Boston, USA	Intraoperative fluorescence imaging	670 or 760 nm LED	150 mm×113 mm	1280 pixel×1024 ×	450	Yes	Clinical trial
GXMI Navigator	Institute of Automation, Beijing, China	Intraoperative fluorescence imaging	760 nm LED	250 mm×250 mm	2456 pixel×2048 pixel	>300	Yes	Clinical trial

NIR-II 手术导航系统因光路更加复杂、对相机要求更高、需要与可见光路兼容等问题,目前仍处于初始研究阶段。中国科学院自动化研究所田捷教授团队研制了首台开放式 NIR-II 手术导航系统,如图 2 所示^[33],并首次完成了人体试验;结果显示:NIR-II 荧光手术导航系统可以在术中检测到其他医学成像设备未能检测到的微小肝癌病灶和转移灶,能明显改善肿瘤的手术切除效果。由于腹腔镜、纤支镜等内镜系统的内部空间狭小,考虑到人体工学等易操作

性,将 NIR-II 相机及其光路与可见光相机及其光路进行兼容、整合尤为困难,甚至需要考虑 NIR-II 光和可见光的光路复用与共享等问题。目前具备 NIR-II 成像功能的内镜系统还在探索阶段,还未见应用于临床研究的相关报道。考虑到内镜微创技术在临床上的广泛普及,具备 NIR-II 荧光手术导航能力的内镜系统,如腹腔镜系统、胃肠镜系统、气管镜系统等,是 NIR-II 荧光手术导航技术临床转化与应用的关键,也是目前亟需突破的瓶颈。

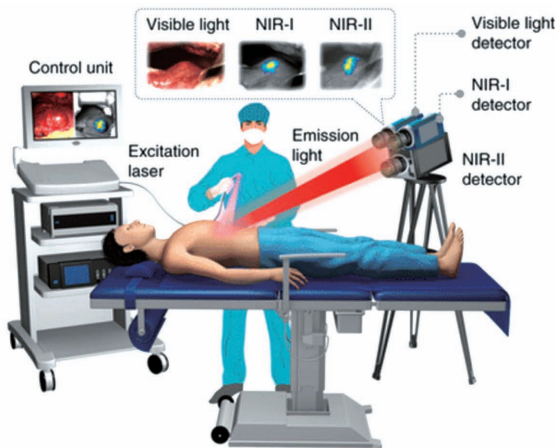


图 2 开放式 NIR-II 荧光手术导航系统^[33]

Fig. 2 Open NIR-II fluorescence surgical navigation system^[33]

3 荧光手术导航探针

目前,被批准用于临床的荧光手术导航探针包括荧光素钠、5-ALA、MB、ICG。其中:荧光素钠无肿瘤特异性,正常组织也可以被染色,组织对荧光素钠发射荧光的吸收和散射比较严重,并且组织的自发荧光会降低对比度,显影效果不佳;5-ALA 需在术前口服,且会使术后皮肤敏感性增加,费用也较高,在肿瘤侵袭区域易出现假阴性,在水肿区域及炎性组织中易出现假阳性^[34];MB 可能会导致心律失常、冠状动脉收缩、心输出量减少、肾血流和肠系膜血流减少以及肺血管压力增加^[35],且用量难以控制。此外,这些荧光探针的激发和发射波长均位于 400~700 nm 区域,穿透深度有限,只能进行组织表面的成像,以致于荧光素钠、5-ALA、MB 在手术导航方面的应用已逐步被临床淘汰。为了获得更深的组织穿透深度、开展更加精准的荧光成像和手术导航,需要使用激发和发射波长更长的近红外荧光探针。目前,荧光手术导航中应用最广泛、研究得最透彻的近红外荧光分子探针是 ICG。ICG 由日本柯达实验室于 1955 年首次合成,可被波长为 750~

810 nm 范围的光激发,激发后发射最大波长为 830 nm 的近红外光,如图 3(a)、(b) 所示^[36]。2009 年,ISHIZAWA 等^[37]首次通过光动态眼成像系统(PDE)将 ICG 用于肿瘤成像,并提出了目前公认的肝脏肿瘤的 ICG 成像机理。在随后的 10 年内,以 ICG 为基础的近红外荧光手术导航技术在肿瘤手术领域得到了广泛应用,诸多临床研究也分别在手术彻底性、手术便捷性、无复发生存和总生存等方面证实了其临床价值,这些临床研究包括乳腺癌前哨淋巴结的指示^[38]、器官切除后血管重建的显示^[39]、脑外科^[40]和消化外科手术中肿瘤位置的显示^[41]等。然而,NIR-I 荧光成像依然存在穿透深度低、背景信号高、信噪比差等一系列固有的瓶颈问题。近年来,随着 NIR-II 荧光成像研究的深入和纳米技术的快速发展,一系列 NIR-II 荧光分子探针,包括有机小分子、有机纳米探针和无机纳米探针,陆续被研发并应用于手术导航领域,而且研究人员针对这些荧光分子探针开发了靶向修饰技术或递送技术,以增加其肿瘤特异性。接下来,本文针对不同类型的 NIR-II 荧光分子探针及其手术导航应用进行简要介绍和分析。

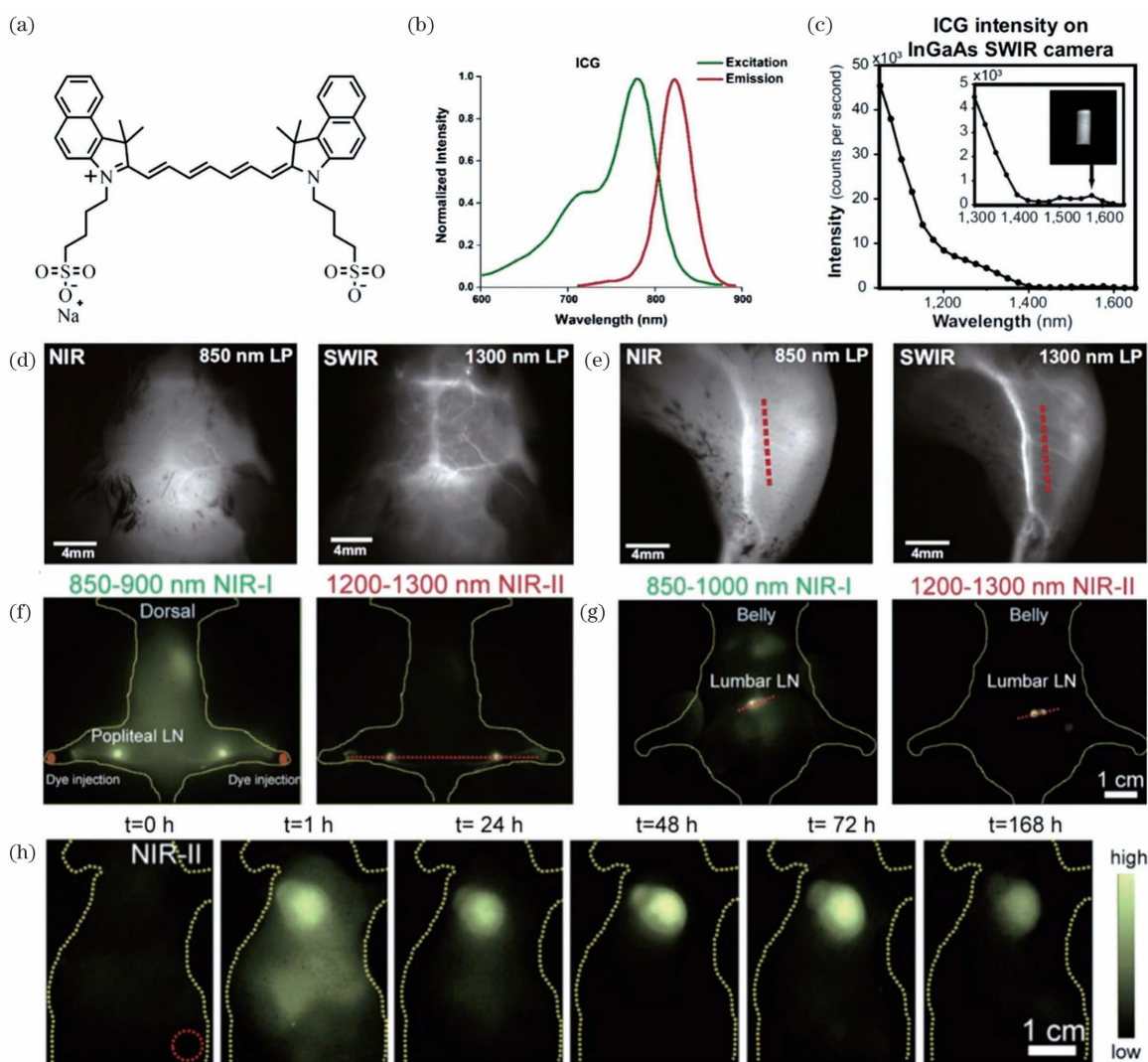


图 3 花菁类染料 ICG 的化学结构式和光谱特性:(a)ICG 的化学结构式;(b)ICG 的激发光谱和 NIR- I 发射光谱^[36];(c)ICG 的 NIR- II 发射光谱^[42]。花菁类染料 ICG 的 NIR- I 和 NIR- II 活体成像效果^[42];(d)小鼠脑部血管成像;(e)小鼠腿部血管成像。(f)~(h)花菁类染料 IR-12N3 作为导航探针在小鼠体内成像^[43]:(f)腿部淋巴结成像;(g)腰椎淋巴结成像;(h)肿瘤成像

Fig. 3 Chemical structural formula and spectral characteristics of ICG: (a) chemical structural formula of ICG; (b) excitation and NIR-I emission spectra of ICG^[36]; (c) NIR-II emission spectrum of ICG^[42]. NIR-I and NIR-II *in vivo* imaging of ICG^[42]: (d) mouse brain vascular imaging; (e) mouse leg vascular imaging. (f)–(h) *in vivo* imaging of IR-12N3 as a navigation probe^[43]: (f) mouse leg lymph nodes imaging; (g) mouse lumbar lymph node imaging; (h) tumor imaging

3.1 有机 NIR- II 荧光手术导航探针

3.1.1 花菁类小分子荧光探针

1857 年, Williams 等^[44]首次合成了花菁染料及其衍生物。花菁染料具有优异的物理化学及光学性质,如高的摩尔消光系数和荧光量子产率、长的荧光发射波长(最大波长可扩展到 NIR- II)等特点^[45-47]。因此,花菁染料被广泛应用于生物医学中的荧光成像领域。进入 21 世纪以后,医学和生命科学的快速发展极大地推动了花菁染料的发展,近年来研究人员开发了很多用于医学成像和手术导航的花菁类荧光分子探针^[48-49]。

在花菁类染料中,最经典的是美国食品药品监督管理局(FDA)批准用于临床的 ICG。到目前为止,ICG 在临床荧光手术导航中的应用是利用其 NIR- I 荧光成像功能。2018 年,麻省理工学院 Bruns 教授课题组^[42]发现,尽管 ICG 的发射光谱在 NIR- I 达到峰值,但是其尾带发射延伸到了 NIR- II,如图 3(c)所示,ICG 在 NIR- II 具有较高的光穿透深度和信噪比,在小动物活体上表现出良好的 NIR- II 成像效果,如图 3(d)、(e)所示。同年,美国国立卫生研究院陈小元教授课题组对现有的 NIR-I 花菁染料进行了系统分析,结果发现:一些量子产率

高、荧光强度大的NIR-II花青染料,如IR-12N3、ICG和IRDye800,在NIR-II区域也具有明亮的尾发射,并具有高的量子产率和摩尔消光系数,从而可以用于小鼠腿部淋巴结[如图3(f)所示]、腰椎淋巴结[如图3(g)所示]以及肿瘤[如图3(h)所示]等模型的NIR-II实时成像;这些探针在NIR-II成像时的穿透深度、分辨率、灵敏度以及信噪比等相比NIR-I成像都获得了显著提升。因此,上述这些花青染料都具有

NIR-II荧光手术导航的潜力^[43]。笔者所在研究团队也于2019年开展了基于ICG的NIR-II荧光手术导航的工作,并在ICG NIR-II荧光成像的引导下实施了小鼠乳腺癌模型的精准手术导航;结果显示:在ICG NIR-II荧光手术导航的引导下,能够在术中实时发现肉眼难以发现的微小转移灶和手术切缘的微小残留,可以显著提升手术切除的精准度和彻底性,如图4(a)所示^[50]。2020年,田捷教授团队^[33]首次完成了ICG

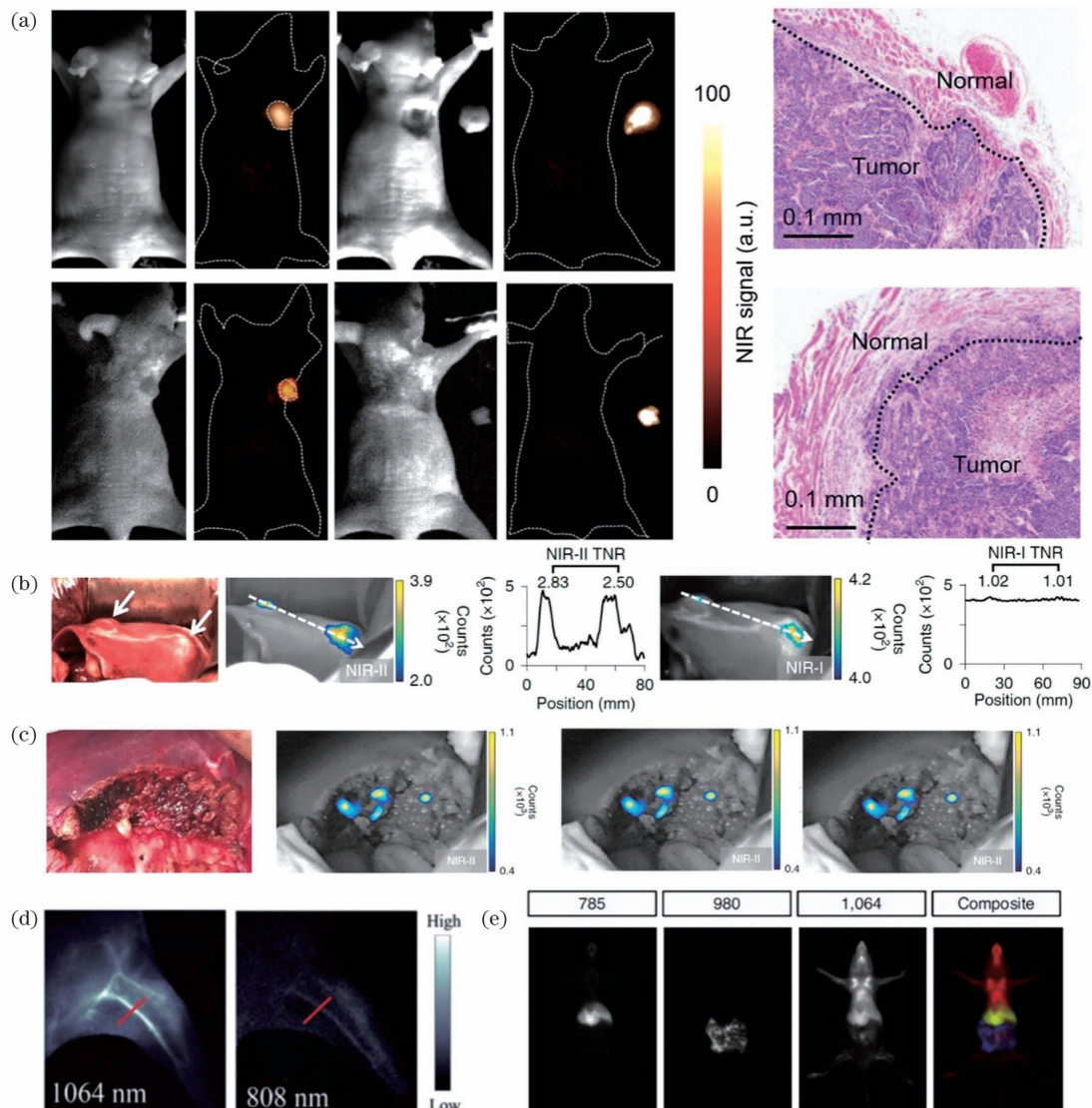


图4 ICG用于NIR-II荧光手术导航:(a)在小鼠乳腺癌模型中,ICG用于NIR-II荧光手术导航引导下的肿瘤切除^[50];在人体试验中,(b)ICG NIR-II成像的信噪比高于NIR-I成像,(c)ICG用于NIR-II荧光手术导航下的肝癌切除^[33]。具有荧光手术导航潜力的NIR-II花青类有机小分子探针用于NIR-II成像;(d)FD-1080在不同激发下的成像效果对比^[51];(e)花青染料Flav衍生物的NIR-II成像^[52]

Fig. 4 NIR-II fluorescence surgical navigation of ICG: (a) tumor resection guided by ICG NIR-II fluorescence surgical navigation in mouse breast cancer model^[50]; in human trials, (b) signal-to-noise ratio of ICG NIR-II imaging is higher than that of NIR-I imaging, (c) liver cancer resection under ICG NIR-II fluorescence surgical navigation^[33]. NIR-II cyanine dyes with fluorescence surgical navigation potential for NIR-II imaging: (d) comparison of imaging effects of FD-1080 under excitation of different wavelengths^[51]; (e) NIR-II imaging of cyanine dye Flav derivative^[52]

NIR-II 荧光成像引导的肝癌手术切除的人体试验,在临幊上证实了该技术可以术中检测到其他医学成像未能检测到的微小肝癌病灶和转移灶,能明显改善手术对肿瘤切除的效果,如图 4(b)、(c)所示。

虽然现有的这些花菁类探针在 NIR-II 的尾带发射也具有良好的成像效果,但其荧光量子产率和穿透深度仍有待提高。为解决这一问题,复旦大学张凡教授团队^[51]合成了一种具有 NIR-II 激发和发射的花菁荧光探针 FD-1080;该探针在加热下能迅速进入胎牛血清(FBS)的疏水空腔内形成蛋白-染料复合物,使得染料单体比例增多和分子刚性结构增大,从而导致其荧光量子产率显著提高到 5.94%;在 1064 nm 激光激发下,该复合物在 1080 nm 处具有很强的荧光发射特性,能实现小鼠下肢的高分辨成像,如图 4(d)所示。加利福尼亚大学 Sletten 教授团队^[52]通过对吸收和发射带较窄的花菁染料 Flav 进行结构改造,合成出 11 个含有不

同取代基的花菁探针;他们从 11 个化合物中筛选出两个性能最好的探针,将其分别匹配 980 nm 和 1064 nm 激发波长,结合临床已批准使用的 ICG,实现了实时、三色的高时空分辨 NIR-II 成像,如图 4(e)所示。这些花菁类探针的开发为 NIR-II 荧光手术导航分子探针提供了更多选择,未来必将成为手术导航技术临床转化的强大推动力。

3.1.2 给体-受体(D-A)型有机小分子荧光探针

在分子设计中,引入电子供体(D)和受体(A)是调整 π 共轭有机化合物电子结构的有效手段。当在小分子荧光探针中引入 D 和 A 后,其能隙会降低,荧光激发和发射光谱也会相应地发生红移。因此,D-A 型 NIR-II 荧光有机小分子也被广泛探索。中国科学院长春应用化学研究所王植源教授课题组^[53]通过使用强电子受体——苯并双(1,2,5-噻二唑)及其衍生物,制备了一系列 D- π -A- π -D 型小分子,如图 5(a)所示,这些小分子在 NIR-II 表现出了

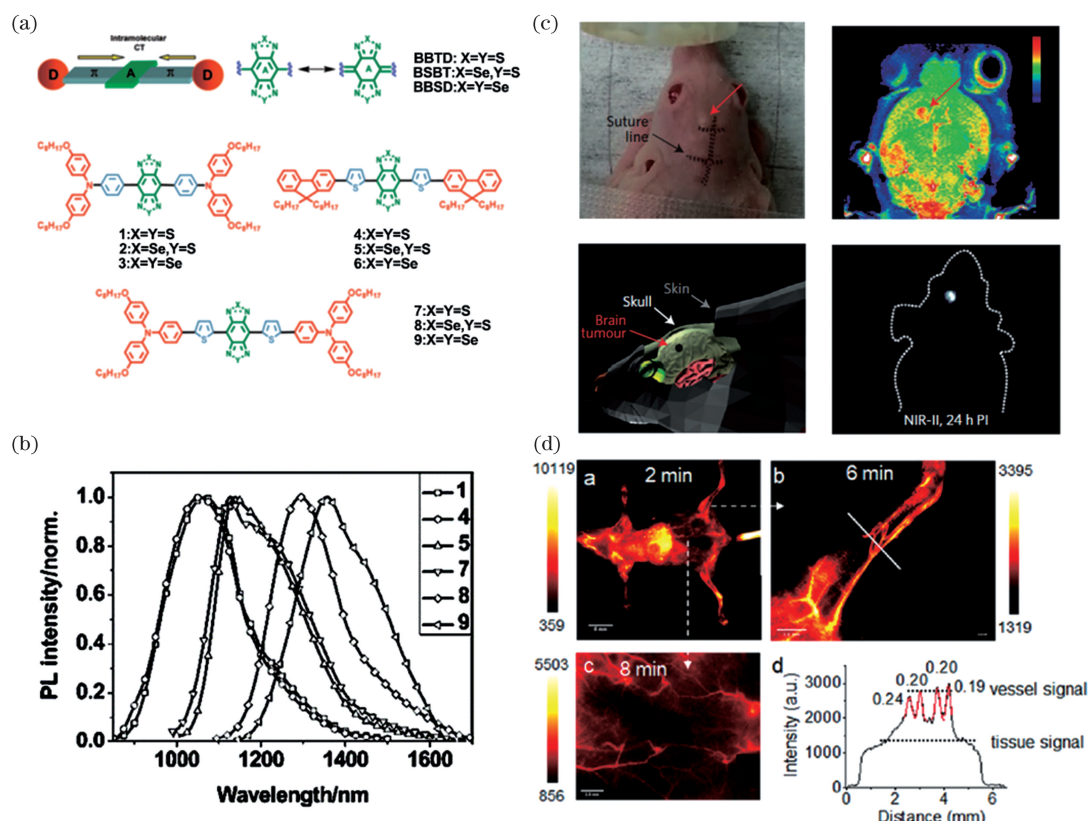


图 5 具有荧光手术导航潜力的 D-A 型有机小分子探针。(a)~(b)D- π -A- π -D 型有机小分子及其荧光发射光谱^[53]; (c) 有机小分子探针 CH1055 在脑胶质瘤模型中的 NIR-II 荧光成像^[54]; (d) 有机小分子探针 FM1210 在小鼠 NIR-II 活体荧光成像中的效果^[56]

Fig. 5 D-A type organic small molecule probe with the potential of fluorescence surgical navigation. (a)–(b) D- π -A- π -D type organic small molecule probe and its fluorescence emission spectrum^[53]; (c) NIR-II fluorescence imaging of small molecule probe CH1055 in brain glioma model^[54]; (d) NIR-II fluorescence *in vivo* imaging of organic small molecule probe FM1210 in mouse^[56]

非常强的荧光发射,如图 5(b)所示。2016 年,斯坦福大学戴宏杰教授团队^[54]报道了一种以苯并双噻二唑(BBTD)作为电子受体(A)、以三苯胺作为电子给体(D),组成 D-A-D 分子骨架的 NIR-II 小分子荧光探针 CH1055,并将其用于脑胶质瘤成像,如图 5(c)所示,但该荧光探针的荧光量子产率很低(仅为 0.2%)。为了达到临床应用的目的,需开发一些高荧光量子产率的 D-A 型 NIR-II 荧光探针。戴宏杰教授团队与南方科技大学梁永晔教授课题组^[55]合作,以 2,6-烷氧基链取代的苯作为电子屏蔽单元,以 3,4-乙烯二氧噻吩(EDOT)作为电子给体单元,用于提高荧光分子在水溶液中的量子产率;并基于上述设计开发出了荧光探针 IR-E1,其荧光发射波长在 900~1400 nm 之间,该荧光探针在水溶液中的量子产率可以达到 0.7%,并被成功应用于小鼠脑震荡模型的 NIR-II 活体荧光成像。然而,这些用于活体成像的苯并双噻二唑衍生物探针的激发和发射波长通常分别位于约 800 nm 和 1000 nm 处,波长仍然较短。中国科学院化学研究所马会民教授课题组^[56]用 Se 原子替代苯并双噻二唑中的 S,制备出了一种发射波长超过 1200 nm 且可用于活体成像的小分子光学探针 FM1210;FM1210 的长波长发射使其能以 100 frame/s 的帧率对小鼠进行高速 NIR-II 活体荧光成像,如图 5(d)所示。这些 NIR-II 荧光分子探针优异的成像性能,为其应用于 NIR-II 荧光手术导航奠定了良好的基础。

3.1.3 有机聚合物纳米探针

有机共轭聚合物由 C—C 和 C=C 交替连接而成,有三个或三个以上互相平行的 P 轨道,从而形成了独特的 π 电子共轭结构,显著缩小了成键和反键能带间的能隙,为载流子和自由电子提供了离域迁移的条件,加之电子或能量可以自由地在共轭骨架上移动,因此,有机共轭聚合物具有半导体性质和特殊的光学性能^[57-60]。由共轭聚合物制成的纳米尺寸的聚合物纳米颗粒具有光谱可调、良好的光稳定性、荧光强度高、生物安全性高和表面易功能化等众多优点,因此在生物医学成像和手术导航领域具有广阔的应用前景。近年来,研究人员合成了一系列具有良好 NIR-II 荧光成像效果的有机聚合物纳米探针。2014 年,斯坦福大学戴宏杰教授课题组^[61]合成了一种荧光聚合物(pDA),并利用磷脂-聚乙二醇对该聚合进行纳米组装,得到了生物相容的 pDA-PEG 纳米探针;该纳米探针的最大发射峰在 1047 nm 处,位于 NIR-II 生物窗口;该聚合物纳米

探针高的量子产率(1.7%)使其可以以 25 frame/s 的速率对小鼠动脉血流、深层组织等进行超快 NIR-II 荧光成像。2019 年,中南大学邹应萍教授课题组^[62]以苯并二噻吩(BDT)作为供体、以三唑[4,5-g]喹喔啉(TQ)作为受体,合成了三种类型的聚合物(P1、P2 和 P3),如图 6(a)所示,并将其组装成聚合物纳米探针(P1-Pdot、P2-Pdot 和 P3-Pdot),这些聚合物纳米探针展示了 NIR-II 荧光发射性能,如图 6(b)所示;随后,他们将 P1-Pdot 应用于小鼠血管[如图 6(c)所示]和荷瘤小鼠肿瘤的 NIR-II 成像,成像结果都表现出高的信噪比。2020 年,南京工业大学黄维院士团队^[63]开发了一种新型的共轭聚合物纳米探针 L1057,并通过显微成像和宏观成像的方式验证了 L057 的活体 NIR-II 荧光成像能力:在脑血管的显微成像中,1.9 μm 的脑血管也能够被清晰成像,且具有较高的信噪比;对开颅鼠进行脑血管成像,最大探测深度高达 900 μm;在小鼠全身血管的成像中,可以清晰地观察到直径约 200 μm 的血管。此外,L1057 对小鼠的微小肿瘤也展示了良好的成像效果,如图 6(d)所示。上述这些有机聚合物纳米探针优异的 NIR-II 荧光成像效果,为其应用于手术导航奠定了基础,未来有望成为 NIR-II 荧光手术导航的新型分子探针。

3.1.4 AIE 荧光纳米探针

用于生物成像、检测与治疗的有机发光材料的应用环境都是水溶液,而现有的大部分荧光探针在聚集态时会由于分子间 π-π 相互作用的增强而出现荧光强度大幅降低的现象,即存在聚集猝灭现象,从而极大地限制了这些探针在生物分子检测、成像和标记中的应用。2001 年,唐本忠院士团队^[64]发现了与聚集猝灭完全相反的聚集诱导发光(AIE)现象:一些分子在聚集或者固态时,其荧光强度显著高于其在溶液中的发光强度。AIE 有机荧光探针具有光稳定性好、信噪比高、生物相容性好等优点,在生物医学成像及手术导航中展现出了巨大的应用潜力^[65-68]。

近年来,研究人员开发了一系列用于 NIR-II 荧光成像的 AIE 荧光纳米探针。2018 年,中国科学院深圳先进技术研究院郑海荣研究员团队^[69]与新加坡国立大学刘斌教授团队合作,构建了 NIR-II (1000~1700 nm) AIE 分子,通过纳米共沉淀技术制备了 RGD 多肽靶向修饰的 AIE 探针 TB1-RGD,并用该探针实现了脑胶质瘤的 NIR-II 荧光成像。南方科技大学李凯教授课题组^[70]开发了一种由疏

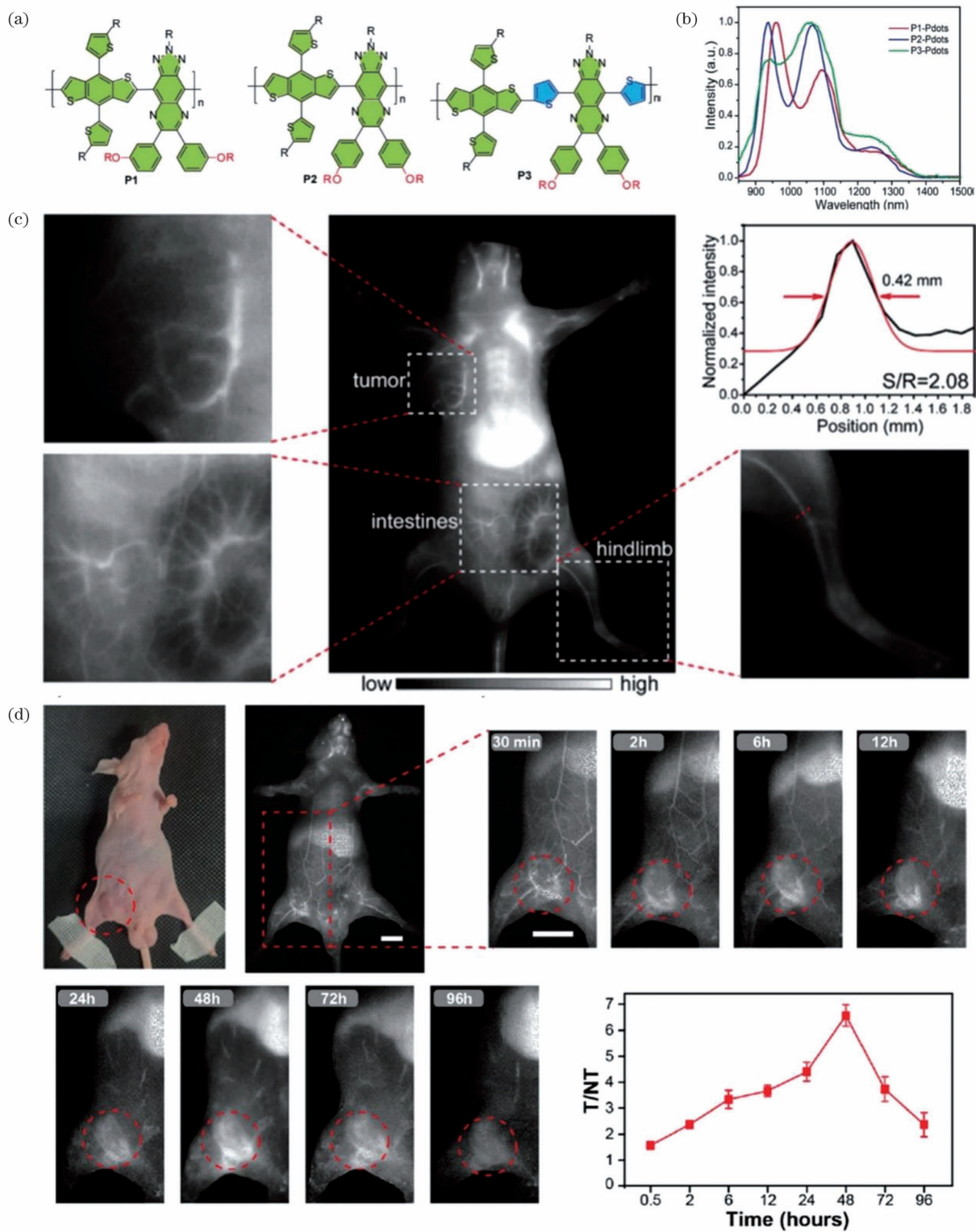


图 6 聚合物纳米探针用于 NIR-II 荧光成像。(a)NIR-II 聚合物 P1、P2、P3 的结构^[62];(b)聚合物 P1、P2、P3 组装的纳米探针 P1-Pdots、P2-Pdots、P3-Pdots 的荧光发射光谱^[62];(c)P1-Pdots 对小鼠血管的 NIR-II 荧光成像^[62];(d)LNIR-II 聚合物纳米探针 L1057 对肿瘤的 NIR-II 荧光成像^[63]

Fig. 6 Polymer nanoprobes for NIR-II fluorescence imaging. (a) Structures of NIR-II polymers P1, P2, and P3^[62]; (b) fluorescence emission spectra of nanoprobe P1-Pdots, P2-Pdots, and P3-Pdots assembled with polymers P1, P2, and P3^[62]; (c) NIR-II fluorescence blood vessels imaging of P1-Pdots^[62]; (d) NIR-II fluorescence tumor imaging of LNIR-II nanoprobe L1057^[63]

水性供体-受体-供体(D-A-D)核心和亲水性聚乙二醇(PEG)链构成的两亲性聚集诱导发光分子组装的纳米探针(SA-TTB-PEG₁₀₀₀)，该探针具有超过1000 nm的最大发射峰和超过10%的荧光量子产率，在小鼠和新西兰兔模型上实现了穿透深度约为1 cm、在体分辨率约为38 μm的多尺度NIR-II荧光成像，如图7(a)、(b)所示。此外，李凯教授团队^[71]合成了基于TTB分子的NIR-II AIE纳米探针，并在灵长类动物体内成功实现了深度高达1.5 cm的血管成像，突

破了当前NIR-II荧光成像深度在毫米级别的限制。2021年，浙江大学钱骏教授团队^[72]提出了长脂链生物可排泄AIE探针设计思路，并将该AIE探针成功应用于非人灵长类动物NIR-II穿颅脑血管荧光成像及NIR-II b区肠胃道荧光造影，如图7(c)、(d)所示。上述AIE纳米探针展示出了良好NIR-II荧光成像效果，为手术导航探针提供了更多选择。然而，如何系统地评价这些聚合物纳米探针的生物安全性，推动其临床转化，仍是目前面临的瓶颈问题之一。

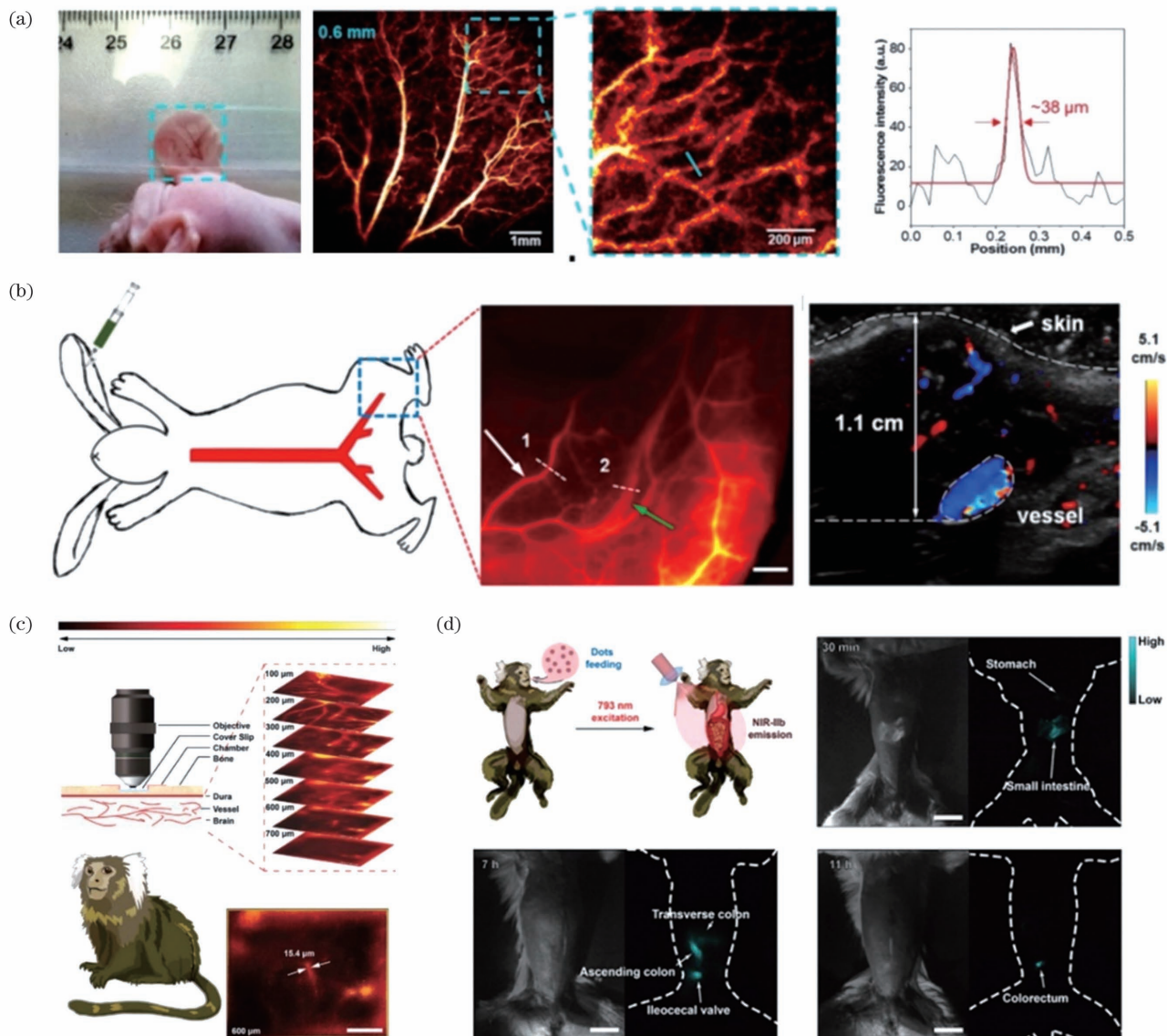


图7 AIE荧光纳米探针的应用。AIE荧光纳米探针SA-TTB-PEG₁₀₀₀用于小鼠(a)和新西兰兔(b)的多尺度NIR-II荧光成像的效果^[70]；AIE纳米探针OTPA-BBT用于非人灵长类动物NIR-II穿颅脑血管荧光成像的效果(c)以及用于近红外NIR-II b区肠胃道荧光造影的效果(d)^[72]

Fig. 7 Application of AIE fluorescent nanoprobe. NIR-II fluorescence imaging of AIE fluorescent nanoprobe SA-TTB-PEG₁₀₀₀ for mouse (a) and New Zealand rabbit (b)^[70]; AIE nanoprobe OTPA-BBT for NIR-II transcranial blood vessel fluorescence imaging in non-human primates (c) and NIR-II b区肠胃道荧光造影 (d)^[72]

3.2 无机荧光纳米探针

3.2.1 无机量子点

量子点是一种球形或类球形的半导体纳米晶材料,其三维尺寸均小于该半导体材料的激子玻尔直径,一般在2~10 nm之间。这类半导体纳米晶可将其电子和空穴限制在三维空间内,这一特性与自然界中的原子或分子类似,因此被称为量子点。量子点材料在特殊波长光的激发下会发出特定波长的荧光,且量子点的吸收光谱、激发光谱和荧光光谱都会随着该半导体纳米晶尺寸以及组成的变化而变化。因此,通过调节量子点的尺寸可以实现对其吸收光谱、激发光谱和荧光发射光谱的精准调节,使其在荧光成像和手术导航等领域有着广阔的应用前景^[73-75]。

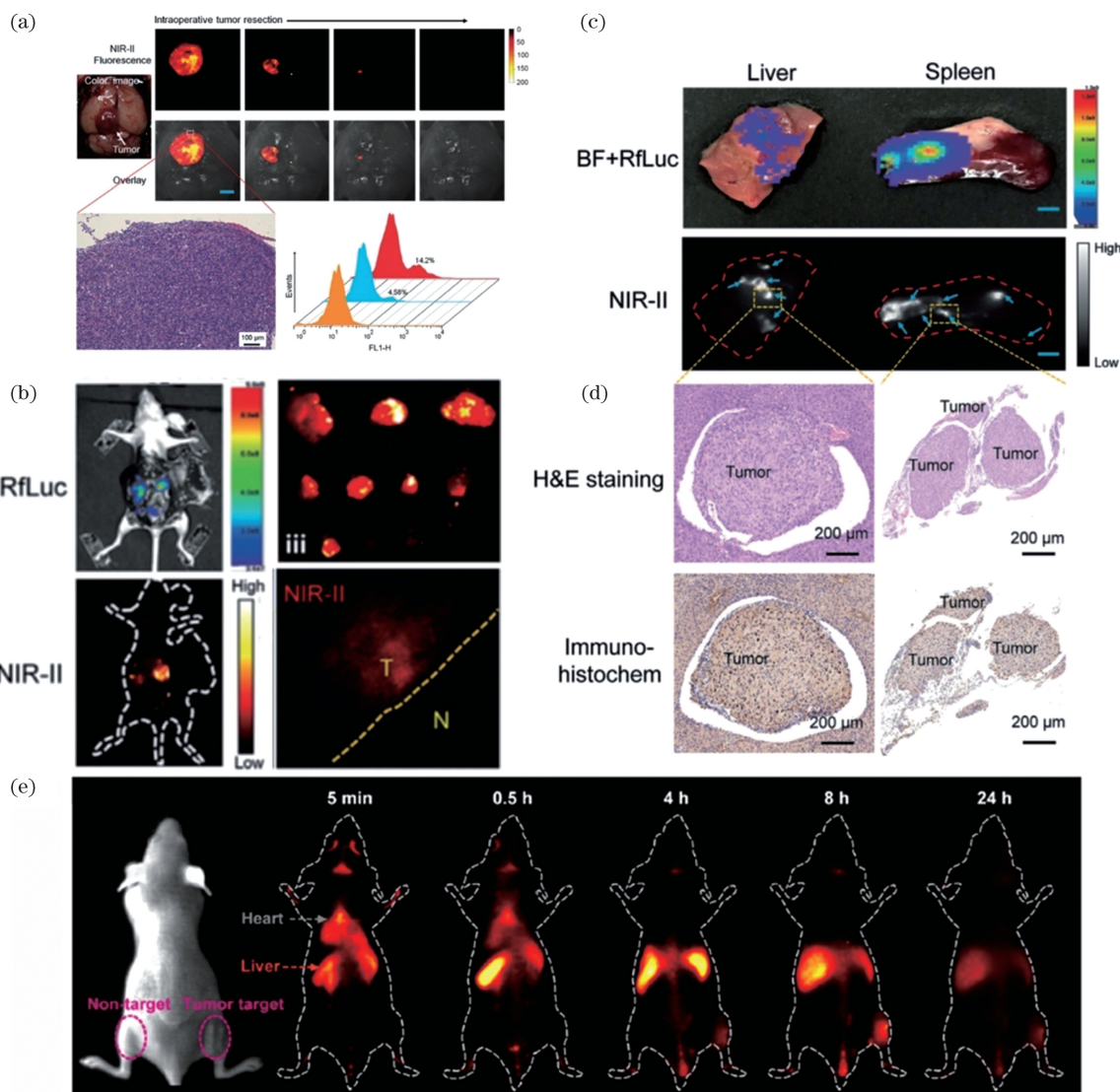


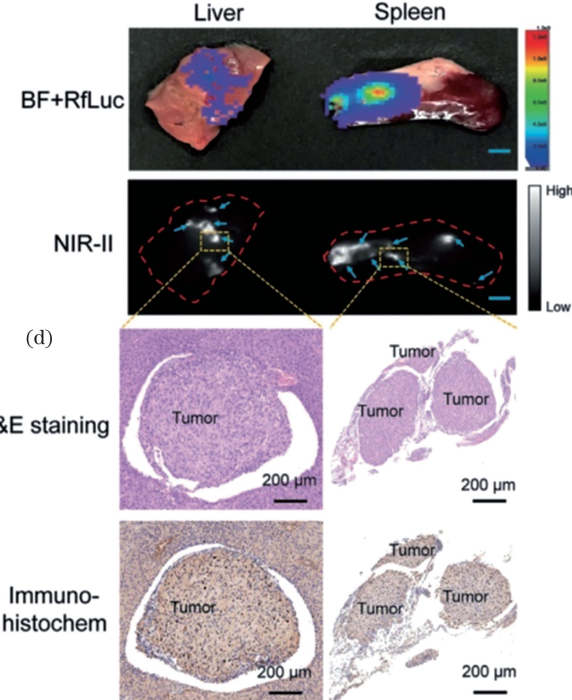
图8 用于NIR-II成像的量子点。(a)Ag₂S纳米探针用于脑胶质瘤^[77]的NIR-II成像和手术导航;(b)~(d)Ag₂S纳米探针用于腹膜转移瘤的NIR-II成像和手术导航^[80];(e)NIR-II量子点CISe用于活体小鼠肿瘤成像^[81]

Fig. 8 Quantum dot for NIR-II imaging. (a) Ag₂S quantum dot for NIR-II imaging and surgical navigation of brain glioma^[77]; (b)–(d) Ag₂S quantum dot for NIR-II imaging and surgical navigation of peritoneal metastases^[80]; (e) CISe quantum dot used for NIR-II tumor imaging^[81]

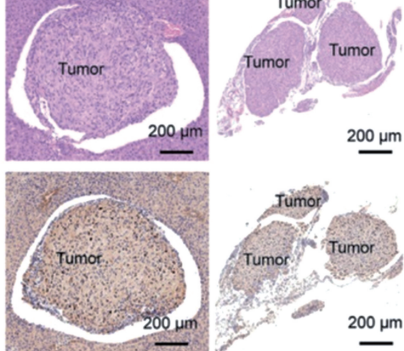
NIR-II荧光量子点具有更长的发射波长,其散射强度与波长的四次方呈反比,因而可以穿透更深的皮肤和血液等生物组织,获得更高的成像分辨率,这使得其在荧光成像和手术导航的应用上具有独特优势。近年来,NIR-II荧光量子点已被广泛开发和应用。

中国科学院苏州纳米技术与纳米仿生研究所王强斌教授团队^[76-79]对近红外区荧光量子点的活体成像开展了系列研究,首次报道了Ag₂S量子点在近红外区的荧光性质,并将其应用于近红外区活体荧光成像,在小动物活体水平上获得了高组织穿透深度(>1.5 cm)、高时间分辨率(约30 ms)和高空间分辨率(约25 μm)的原位、实时成像。同时,他们还将Ag₂S量子点分别应用于脑胶质瘤[如图8(a)所

(c)



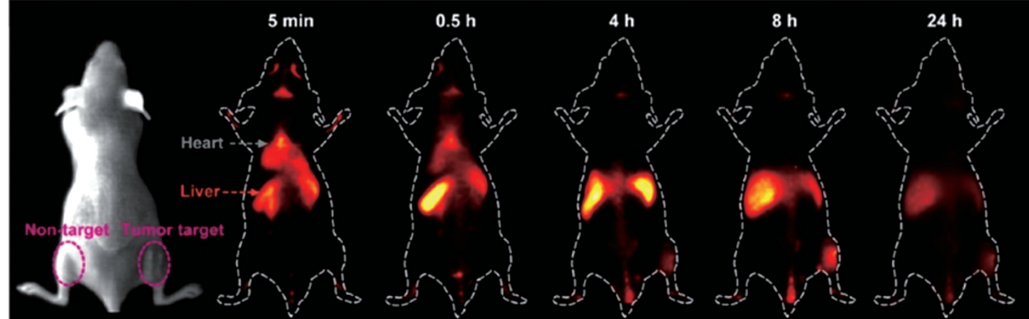
(d)



Tumor
Tumor
Tumor
Tumor

200 μm
200 μm
200 μm
200 μm

(e)



示]^[77] 和乳腺癌转移瘤[如图 8(b)~(d) 所示]^[80] 的 NIR-II 荧光手术导航,显著提高了手术切除的精准度和彻底性。中国科学院福建物质结构研究所陈学元教授团队^[81] 开发了一种新型 NIR-II 荧光量子点 CuInSe₂ (CISe),他们通过调节量子点中 Se 和 In 的掺杂比例,将其最大发射长从 920 nm 调节到 1224 nm;当 CISe 采用 ZnS 包覆后,稳定性明显提高,且其在 NIR-II 的绝对荧光量子产率能达到 21.8%。值得注意的是,该量子点对微小肿瘤表现出了良好的 NIR-II 荧光成像效果[如图 8(e)所示]。这些 NIR-II 荧光量子点的开发及其在小动物活体水平上表现出的良好的荧光成像效果,为其应用于 NIR-II 荧光手术导航奠定了基础。

3.2.2 稀土纳米探针

稀土元素是 17 种特殊元素的总称,包括化学元素周期表中镧系的 15 个元素以及与镧系密切相关的钇(Y)和钪(Sc)这两种元素。稀土离子因具有独特的电子结构及丰富的能级,能产生紫外光到近红外光等各种波长的发射,展现出了良好的光学特性。其中,稀土荧光材料以其宽的荧光发射光谱、高的荧光量子效率、良好的荧光稳定性以及低的生物毒性等优点,在分析检测和生物医学成像等方面显示出了极大的应用潜能和广阔的应用前景^[82-85]。一直以来,科研工作者对稀土纳米探针的研究主要集中在可见光到 NIR-I 波段,但其荧光量子产率和穿透深度偏低,从而限制了其在荧光手术导航上的应用。

近年来,NIR-II 稀土纳米探针也陆续被科研工作者开发,并被成功应用到荧光手术导航领域。2018 年,复旦大学张凡教授课题组^[86] 开发了一种稀土掺杂的下转换纳米探针 (DCNPs-L₁-FSH_β/DCNPs-L₂-FSH_β),并结合化学自组装技术实现了该探针在肿瘤内的长期稳定标记,极大地提高了光学成像的信噪比,成功实现了卵巢癌腹膜转移以及淋巴结转移肿瘤在 NIR-II 荧光成像引导下的精准切除,如图 9(a)~(c) 所示。哈尔滨工业大学陈冠英教授课题组^[87] 采用材料晶相和核壳结构精准调控策略,制备了一种发射波长在 1525 nm、位于 NIR-IIb (1500~1700 nm) 区域的小尺寸 (7.4 nm) NaErF₄ 稀土纳米晶,该纳米晶在小鼠体内能被快速代谢清除,在小鼠全身血管的高分辨动态 NIR-II 荧光成像中展现出了良好的效果。2021 年,南方医科大学方驰华教授课题组^[88] 联合中国科学院自动化所田捷教授课题组报道了一种新型多功能 NIR-II 下转换稀土纳米探针 NPs@Lips,其在 808 nm 激光激发

下,可以同时发射三种不同谱段的荧光信号,这三个谱段分别为 1000~1100 nm (NIR-II)、1300~1350 nm (NIR-IIa) 和 1500~1700 nm (NIR-IIb);该探针经脂质体修饰后,能快速从肝脾排出,具有良好的生物相容性;利用该探针可在术中对肠道血管进行多谱段 NIR-II 荧光成像[如图 9(e)所示],以区分正常和异常血管,并可以实现小鼠淋巴结的精准定位和 NIR-II 荧光引导下的淋巴结切除。虽然 NIR-II 稀土纳米探针在小动物活体荧光手术导航上的应用上具有良好的效果,但稀土元素的体内代谢途径和生物安全性还缺乏系统的研究数据。进一步的代谢途径和安全性的系统研究,是其临床转化的基础。

3.2.3 单壁碳纳米管

单壁碳纳米管(SWNTs)是一种由单层石墨卷成的柱状无缝管,其直径为 0.7~2 nm。SWNTs 具有长径比大、结构缺陷小、端部曲率半径小等特点,这些特点使其表现出了良好的光学性能;其荧光发射大多位于近红外区域,并且具有光稳定性、无光漂白等优点,这使得其在 NIR-II 荧光成像和荧光手术导航领域展现出了巨大的应用潜力。2009 年,斯坦福大学戴宏杰教授团队^[89] 首先发现 SWNTs 可发射 NIR-II 荧光,并通过对其表面进行磷脂-聚乙二醇 (PL-PEG) 修饰提高了它的水溶性和生物相容性,然后成功地将 SWNTs 用于 NIR-II 小鼠活体荧光成像。2014 年,他们团队进一步利用 SWNTs 在 1300~1400 nm 的固有发射,在不开颅的情况下,实现了脑穿透深度 > 2 mm、空间分辨率达 10 μm 的无创脑血管 NIR-II 荧光成像^[90]。随后,他们团队还研发了一种荧光亮度显著增强的半导体型 SWNTs,其在 808 nm 激光激发下的发射波长可以达到 1500~1700 nm,同时他们成功地将该 SWNTs 用于活体小鼠毛细血管和肿瘤的 NIR-II 荧光成像^[91]。SWNTs 良好的 NIR-II 荧光成像效果为其在手术导航方面的应用奠定了基础。

3.3 荧光手术导航探针的靶向修饰

目前,ICG 已被广泛应用于临床荧光手术导航。但是,ICG 是基于肿瘤组织与正常组织对其代谢的差异进行术中成像的,从而导致其在多数肿瘤组织中无法有效富集,使其术中成像的信噪比较低,最终影响术中成像和手术导航的效果。因此,科研工作者致力于与临床医生紧密合作,基于受体介导的特异靶向原理开发用于手术导航的新型靶向荧光探针。肿瘤细胞表面通常会表达一系列特异的受体,这些受体在肿瘤的生长中起着关键作用。因此,将

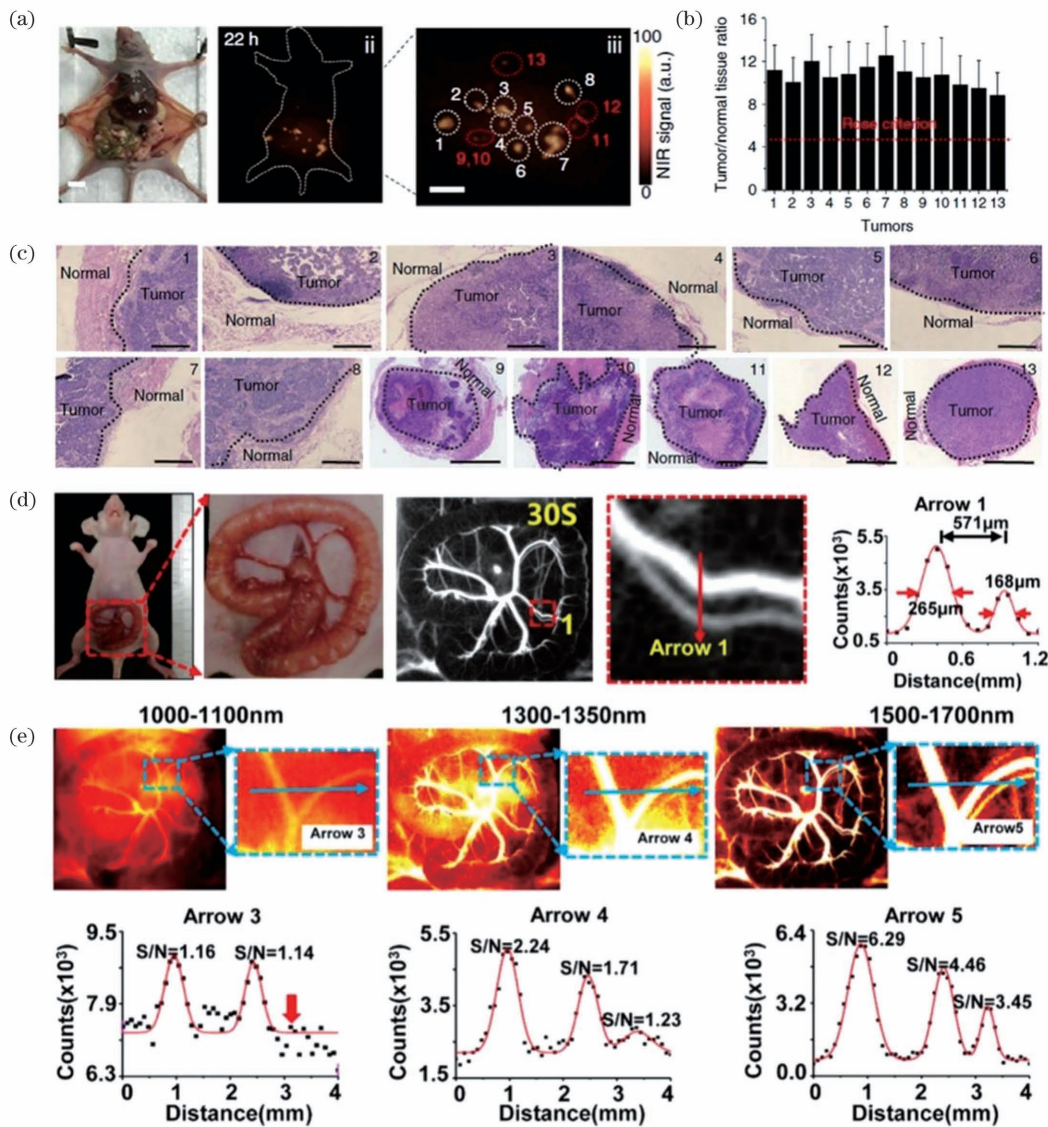


图 9 稀土纳米探针用于 NIR-II 成像。(a)~(b) DCNPs-L₁-FSH_β/DCNPs-L₂-FSH_β 在卵巢癌腹腔转移瘤 NIR-II 成像中的应用^[86]; (c) DCNPs-L₁-FSH_β/DCNPs-L₂-FSH_β 在手术导航中的应用效果展示^[86]; (d) NPs@Lips 用于肠道 NIR-II b 成像^[88]; (e) NPs@Lips 用于术中肠道血管多谱段成像^[88]

Fig. 9 Rare earth nanoprobes for NIR-II imaging. (a)–(b) DCNPs-L₁-FSH_β/DCNPs-L₂-FSH_β for NIR-II imaging in ovarian cancer metastasis model^[86]; (c) DCNPs-L₁-FSH_β/DCNPs-L₂-FSH_β for fluorescence surgical navigation effect display^[86]; (d) NPs@Lips for intestinal NIR-II b imaging^[88]; (e) NPs@Lips for intraoperative multispectral imaging of intestinal vessels^[88]

这些受体作为肿瘤成像的靶点可以提高成像特异性。这类靶点的配体主要包括抗体、多肽和小分子化合物等。武汉大学洪学传教授团队^[92]将靶向乳腺癌细胞表面核仁素的靶向多肽 F3 与 NIR-II 荧光探针 CH1055 偶联, 获得了特异靶向乳腺癌的 NIR-II 荧光探针 CH1055-F3; 该探针可以对移植和原发性乳腺癌模型进行特异的 NIR-II 荧光成像, 并成功引导了小鼠自发乳腺癌的精准手术切除。中国科学院苏州纳米技术与纳米仿生研究所王强斌教授

团队^[80]构建了一种 RGD 多肽偶联的 Ag₂S 量子点探针 APP-Ag₂S-RGD。在构建的小鼠腹膜转移瘤模型中, 该探针实现了微小(0.2 mm)肿瘤的精准 NIR-II 荧光成像和检出; 同时, 在 NIR-II 荧光成像引导下, 该团队利用该探针实现了腹膜转移瘤的精准手术切除。

目前, 也有部分受体介导的肿瘤特异靶向配体修饰的荧光探针进入了临床试验阶段。肿瘤表皮生长因子受体(EGFR)是一种跨膜糖蛋白, 具有配体

诱导的酪氨酸蛋白激酶活性,在胃癌、乳腺癌、膀胱癌和头颈部鳞癌中都会过表达。荷兰格罗宁根大学Nagengast教授团队^[93]将能够特异结合EGFR的帕尼单抗和西妥昔单抗与IRDye800CW荧光探针偶联,制备了肿瘤特异靶向的荧光探针。目前,该探针正在头颈癌(NCT01987375、NCT02415881)荧光手术导航中进行临床评估,期望早日获得阳性结果。此外,以血管生成因子为靶点的贝伐珠单抗偶联的IRDye800CW荧光手术导航探针,在乳腺癌和结直肠癌(NCT01508572、NCT02583568、NCT01691391)上的临床试验也在陆续开展中^[94-95]。这些靶向设计和修饰策略,可以进一步提高荧光手术导航探针的肿瘤靶向特异性,进而提高手术导航的精准性和手术切除的彻底性,为荧光手术导航的进一步临床推广和应用提供支撑。

4 结束语

外科手术中手术边界的精准定位、微小病灶的发现、手术路径的规划等,对于提高手术的精准度、安全性及彻底性至关重要。术中实时荧光手术导航为精准外科提供了新工具,使临床医生可以在术中更加精准地区分病灶边界、识别残余和微小病灶、发现重要的管道与神经结构,进而提高手术的安全性和彻底性,保障病人的预后和远期生存。目前,已在临幊上应用的NIR-I荧光手术导航技术,极大地提高了外科医生手术的精准性,但也仍面临着穿透深度小、背景信号强、信噪比低、无病灶特异性等一系列瓶颈问题。近年来,NIR-II荧光成像技术的快速发展,为解决上述瓶颈问题提供了新的机遇和手段。随着仪器科学、材料科学、化学与光学等多个学科的交叉融合,科研人员已经研制出了一系列NIR-II荧光手术导航设备和分子探针。对于这些设备和探针的临幊转化,构建一致性高、与人体肿瘤发生发展背景高度相近的动物模型是目前面临的重要瓶颈问题之一。此外,探针的长研发周期和低收益导致的投入不足也是目前遇到的瓶颈问题。因此,进一步推动NIR-II荧光手术导航的临幊转化需要企业、医院、临幊医生和基础研究人员的共同参与。目前,一些临幊前研究已经显示出良好的临幊前景,为进一步推动NIR-II荧光手术导航的转化应用奠定了基础,未来必将为精准外科手术时代的来临提供强有力保障。

参 考 文 献

- [1] Sung H, Ferlay J, Siegel R L, et al. Global cancer statistics 2020: GLOBOCAN estimates of incidence and mortality worldwide for 36 cancers in 185 countries[J]. CA: a Cancer Journal for Clinicians, 2021, 71(3): 209-249.
- [2] Moran M S, Schnitt S J, Giuliano A E, et al. Society of Surgical Oncology-American Society for radiation oncology consensus guideline on margins for breast-conserving surgery with whole-breast irradiation in stages I and II invasive breast cancer[J]. Annals of Surgical Oncology, 2014, 21(3): 704-716.
- [3] de Carvalho A C, Kowalski L P, Campos A H J F M, et al. Clinical significance of molecular alterations in histologically negative surgical margins of head and neck cancer patients[J]. Oral Oncology, 2012, 48(3): 240-248.
- [4] Aliperti L A, Predina J D, Vachani A, et al. Local and systemic recurrence is the achilles heel of cancer surgery[J]. Annals of Surgical Oncology, 2011, 18(3): 603-607.
- [5] Vahrmeijer A L, Hutteman M, van der Vorst J R, et al. Image-guided cancer surgery using near-infrared fluorescence[J]. Nature Reviews Clinical Oncology, 2013, 10(9): 507-518.
- [6] Hameed S, Dai Z. Near-infrared fluorescence probes for surgical navigation [J]. Materials Today Chemistry, 2018, 10: 90-103.
- [7] van Beurden F, van Willigen D M, Vojnovic B, et al. Multi-wavelength fluorescence in image-guided surgery, clinical feasibility and future perspectives [J]. Molecular Imaging, 2020, 19: 1536012120962333.
- [8] Ni X, Zhang X Y, Duan X C, et al. Near-infrared afterglow luminescent aggregation-induced emission dots with ultrahigh tumor-to-liver signal ratio for promoted image-guided cancer surgery [J]. Nano Letters, 2019, 19(1): 318-330.
- [9] Chen T, Su L C, Ge X G, et al. Dual activated NIR-II fluorescence and photoacoustic imaging-guided cancer chemo-radiotherapy using hybrid plasmonic-fluorescent assemblies[J]. Nano Research, 2020, 13(12): 3268-3277.
- [10] Takeuchi M, Sugie T, Abdelazeem K, et al. Lymphatic mapping with fluorescence navigation using indocyanine green and axillary surgery in patients with primary breast cancer[J]. The Breast Journal, 2012, 18(6): 535-541.
- [11] Takada M, Takeuchi M, Suzuki E, et al. Real-time navigation system for sentinel lymph node biopsy in breast cancer patients using projection mapping with indocyanine green fluorescence [J]. Breast Cancer, 2018, 25(6): 650-655.

- [12] Kim D W, Jeong B, Shin I H, et al. Sentinel node navigation surgery using near-infrared indocyanine green fluorescence in early gastric cancer[J]. *Surgical Endoscopy*, 2019, 33(4): 1235-1243.
- [13] Kim M, Son S Y, Cui L H, et al. Real-time vessel navigation using indocyanine green fluorescence during robotic or laparoscopic gastrectomy for gastric cancer[J]. *Journal of Gastric Cancer*, 2017, 17(2): 145-153.
- [14] Kokudo N, Ishizawa T. Clinical application of fluorescence imaging of liver cancer using indocyanine green[J]. *Liver Cancer*, 2012, 1(1): 15-21.
- [15] Nishino H, Hatano E, Seo S, et al. Real-time navigation for liver surgery using projection mapping with indocyanine green fluorescence: development of the novel medical imaging projection system [J]. *Annals of Surgery*, 2018, 267(6): 1134-1140.
- [16] Yahata H, Kobayashi H, Sonoda K, et al. Prognostic outcome and complications of sentinel lymph node navigation surgery for early-stage cervical cancer [J]. *International Journal of Clinical Oncology*, 2018, 23(6): 1167-1172.
- [17] Xiao S Y, Zhang J, Zhu Z Q, et al. Application of fluorescein sodium in breast cancer brain-metastasis surgery [J]. *Cancer Management and Research*, 2018, 10: 4325-4331.
- [18] van Manen L, Handgraaf H J M, Diana M, et al. A practical guide for the use of indocyanine green and methylene blue in fluorescence-guided abdominal surgery[J]. *Journal of Surgical Oncology*, 2018, 118(2): 283-300.
- [19] van der Vorst J R, Vahrmeijer A L, Hutmacher M, et al. Near-infrared fluorescence imaging of a solitary fibrous tumor of the pancreas using methylene blue [J]. *World Journal of Gastrointestinal Surgery*, 2012, 4(7): 180-184.
- [20] Schucht P, Beck J, Abu-Isa J, et al. Gross total resection rates in contemporary glioblastoma surgery: results of an institutional protocol combining 5-aminolevulinic acid intraoperative fluorescence imaging and brain mapping[J]. *Neurosurgery*, 2012, 71(5): 927-936.
- [21] Isomoto H, Nanashima A, Senoo T, et al. *In vivo* fluorescence navigation of gastric and upper gastrointestinal tumors by 5-aminolevulinic acid mediated photodynamic diagnosis with a laser-equipped video image endoscope[J]. *Photodiagnosis and Photodynamic Therapy*, 2015, 12(2): 201-208.
- [22] Kusano M, Tajima Y, Yamazaki K, et al. Sentinel node mapping guided by indocyanine green fluorescence imaging: a new method for sentinel node navigation surgery in gastrointestinal cancer [J]. *Digestive Surgery*, 2008, 25(2): 103-108.
- [23] Hirche C, Mohr Z, Kneif S, et al. Ultrastaging of colon cancer by sentinel node biopsy using fluorescence navigation with indocyanine green [J]. *International Journal of Colorectal Disease*, 2012, 27(3): 319-324.
- [24] Zhang P, Luo H L, Zhu W, et al. Real-time navigation for laparoscopic hepatectomy using image fusion of preoperative 3D surgical plan and intraoperative indocyanine green fluorescence imaging [J]. *Surgical Endoscopy*, 2020, 34(8): 3449-3459.
- [25] Shi Y B, Yuan W, Liu Q Y, et al. Development of polyene-bridged hybrid rhodamine fluorophores for high-resolution NIR-II imaging [J]. *ACS Materials Letters*, 2019, 1(4): 418-424.
- [26] Lei Z H, Sun C X, Pei P, et al. Stable, wavelength-tunable fluorescent dyes in the NIR-II region for *in vivo* high-contrast bioimaging and multiplexed biosensing[J]. *Angewandte Chemie*, 2019, 58(24): 8166-8171.
- [27] Chi C W, Du Y, Ye J Z, et al. Intraoperative imaging-guided cancer surgery: from current fluorescence molecular imaging methods to future multi-modality imaging technology[J]. *Theranostics*, 2014, 4(11): 1072-1084.
- [28] Fengler J. Near-infrared fluorescence laparoscopy: technical description of PINPOINT® a novel and commercially available system [J]. *Colorectal Disease*, 2015, 17(S3): 3-6.
- [29] Gurtner G C, Jones G E, Neligan P C, et al. Intraoperative laser angiography using the SPY system: review of the literature and recommendations for use [J]. *Annals of Surgical Innovation and Research*, 2013, 7(1): 1.
- [30] Guo J H, Gao Y S, Li H Z, et al. Hemodynamic assessment with SPY-indocyanine green angiography in expansion period: a study for expansion capsule pressure optimization[J]. *The Journal of Craniofacial Surgery*, 2018, 29(3): 578-583.
- [31] Muallem M Z, Sayasneh A, Armbrust R, et al. Sentinel lymph node staging with indocyanine green for patients with cervical cancer: the safety and feasibility of open approach using SPY-PHI technique [J]. *Journal of Clinical Medicine*, 2021, 10(21): 4849.
- [32] He K S, Hong X P, Chi C W, et al. A new method of near-infrared fluorescence image-guided hepatectomy for patients with hepatolithiasis: a randomized controlled trial[J]. *Surgical Endoscopy*, 2020, 34(11): 4975-4982.

- [33] Hu Z H, Fang C, Li B, et al. First-in-human liver-tumour surgery guided by multispectral fluorescence imaging in the visible and near-infrared-I / II windows[J]. *Nature Biomedical Engineering*, 2020, 4(3): 259-271.
- [34] Schebesch K M, Brawanski A, Hohenberger C, et al. Fluorescein sodium-guided surgery of malignant brain tumors: history, current concepts, and future project[J]. *Turkish Neurosurgery*, 2016, 26(2): 185-194.
- [35] Dhawan R, Chaney M A. Anesthetic management and hemodynamic management [M]//Raman J. Management of heart failure. London: Springer, 2016: 257-268.
- [36] Almarhaby A M, Lees J E, Bugby S L, et al. Characterisation of a near-infrared (NIR) fluorescence imaging systems intended for hybrid gamma-NIR fluorescence image guided surgery[J]. *Journal of Instrumentation*, 2019, 14(7): P07007.
- [37] Ishizawa T, Fukushima N, Shibahara J, et al. Real-time identification of liver cancers by using indocyanine green fluorescent imaging[J]. *Cancer*, 2009, 115(11): 2491-2504.
- [38] Mieog J S D, Troyan S L, Hutteman M, et al. Toward optimization of imaging system and lymphatic tracer for near-infrared fluorescent sentinel lymph node mapping in breast cancer[J]. *Annals of Surgical Oncology*, 2011, 18(9): 2483-2491.
- [39] Shimada Y, Okumura T, Nagata T, et al. Usefulness of blood supply visualization by indocyanine green fluorescence for reconstruction during esophagectomy [J]. *Esophagus: Official Journal of the Japan Esophageal Society*, 2011, 8(4): 259-266.
- [40] Charalampaki P, Nakamura M, Athanasopoulos D, et al. Confocal-assisted multispectral fluorescent microscopy for brain tumor surgery[J]. *Frontiers in Oncology*, 2019, 9: 583.
- [41] Franz M, Arend J, Wolff S, et al. Tumor visualization and fluorescence angiography with indocyanine green (ICG) in laparoscopic and robotic hepatobiliary surgery—valuation of early adopters from Germany[J]. *Innovative Surgical Sciences*, 2021, 6(2): 59-66.
- [42] Carr J A, Franke D, Caram J R, et al. Shortwave infrared fluorescence imaging with the clinically approved near-infrared dye indocyanine green [J]. *Proceedings of the National Academy of Sciences of the United States of America*, 2018, 115(17): 4465-4470.
- [43] Zhu S, Hu Z, Tian R, et al. Repurposing cyanine NIR-I dyes accelerates clinical translation of near-infrared-II (NIR-II) bioimaging [J]. *Advanced Materials*, 2018, 30(34): 1802546.
- [44] Williams C G. XXVI: researches on chinoline and its homologues[J]. *Transactions of the Royal Society of Edinburgh*, 1857, 21(3): 377-401.
- [45] Shindy H A. Fundamentals in the chemistry of cyanine dyes: a review [J]. *Dyes and Pigments*, 2017, 145: 505-513.
- [46] Constantin T P, Silva G L, Robertson K L, et al. Synthesis of new fluorogenic cyanine dyes and incorporation into RNA fluoromodules[J]. *Organic Letters*, 2008, 10(8): 1561-1564.
- [47] Petty J T, Bordelon J A, Robertson M E. Thermodynamic characterization of the association of cyanine dyes with DNA[J]. *The Journal of Physical Chemistry B*, 2000, 104(30): 7221-7227.
- [48] Sun W, Guo S G, Hu C, et al. Recent development of chemosensors based on cyanine platforms [J]. *Chemical Reviews*, 2016, 116(14): 7768-7817.
- [49] Huang F, Li Y H, Liu J L, et al. Intraperitoneal injection of cyanine-based nanomicelles for enhanced near-infrared fluorescence imaging and surgical navigation in abdominal tumors[J]. *ACS Applied Bio Materials*, 2021, 4(7): 5695-5706.
- [50] Wang P Y, Wang X D, Luo Q, et al. Fabrication of red blood cell-based multimodal theranostic probes for second near-infrared window fluorescence imaging-guided tumor surgery and photodynamic therapy[J]. *Theranostics*, 2019, 9(2): 369-380.
- [51] Li B H, Lu L F, Zhao M Y, et al. An efficient 1064 nm NIR-II excitation fluorescent molecular dye for deep-tissue high-resolution dynamic bioimaging [J]. *Angewandte Chemie*, 2018, 57(25): 7483-7487.
- [52] Cosco E D, Spearman A L, Ramakrishnan S, et al. Shortwave infrared polymethine fluorophores matched to excitation lasers enable non-invasive, multicolour *in vivo* imaging in real time[J]. *Nature Chemistry*, 2020, 12(12): 1123-1130.
- [53] Qian G, Dai B, Luo M, et al. Band gap tunable, donor-acceptor-donor charge-transfer heteroquinoid-based chromophores: near infrared photoluminescence and electroluminescence[J]. *Chemistry of Materials*, 2008, 20(19): 6208-6216.
- [54] Antaris A L, Chen H, Cheng K, et al. A small-molecule dye for NIR-II imaging [J]. *Nature Materials*, 2016, 15(2): 235-242.
- [55] Zhang X D, Wang H, Antaris A L, et al. Traumatic brain injury imaging in the second near-infrared window with a molecular fluorophore[J]. *Advanced Materials*, 2016, 28(32): 6872-6879.

- [56] Fang Y, Shang J Z, Liu D K, et al. Design, synthesis, and application of a small molecular NIR-II fluorophore with maximal emission beyond 1200 nm [J]. *Journal of the American Chemical Society*, 2020, 142(36): 15271-15275.
- [57] Li J C, Pu K Y. Development of organic semiconducting materials for deep-tissue optical imaging, phototherapy and photoactivation [J]. *Chemical Society Reviews*, 2019, 48(1): 38-71.
- [58] Lyu Y, Xie C, Chechetka S A, et al. Semiconducting polymer nanobioconjugates for targeted photothermal activation of neurons [J]. *Journal of the American Chemical Society*, 2016, 138(29): 9049-9052.
- [59] Cao Z Y, Feng L Z, Zhang G B, et al. Semiconducting polymer-based nanoparticles with strong absorbance in NIR-II window for *in vivo* photothermal therapy and photoacoustic imaging [J]. *Biomaterials*, 2018, 155: 103-111.
- [60] Liang G H, Xing D. Progress in organic nanomaterials for laser-induced photothermal therapy of tumor [J]. *Chinese Journal of Lasers*, 2018, 45(2): 0207020.
梁国海, 邢达. 用于肿瘤光热治疗的有机纳米材料研究进展 [J]. *中国激光*, 2018, 45(2): 0207020.
- [61] Hong G S, Zou Y P, Antaris A L, et al. Ultrafast fluorescence imaging *in vivo* with conjugated polymer fluorophores in the second near-infrared window [J]. *Nature Communications*, 2014, 5: 4206.
- [62] Liu Y, Liu J F, Chen D D, et al. Quinoxaline-based semiconducting polymer dots for *in vivo* NIR-II fluorescence imaging [J]. *Macromolecules*, 2019, 52(15): 5735-5740.
- [63] Yang Y Q, Fan X X, Li L, et al. Semiconducting polymer nanoparticles as theranostic system for near-infrared-II fluorescence imaging and photothermal therapy under safe laser fluence [J]. *ACS Nano*, 2020, 14(2): 2509-2521.
- [64] Luo J, Xie Z, Lam J W, et al. Aggregation-induced emission of 1-methyl-1, 2, 3, 4, 5-pentaphenylsilole [J]. *Chemical Communications*, 2001(18): 1740-1741.
- [65] Chen S J, Liu J Z, Liu Y, et al. An AIE-active hemicyanine fluorogen with stimuli-responsive red/blue emission: extending the pH sensing range by “switch + knob” effect [J]. *Chemical Science*, 2012, 3(6): 1804-1809.
- [66] Dong Z Z, Bi Y Z, Cui H R, et al. AIE supramolecular assembly with FRET effect for visualizing drug delivery [J]. *ACS Applied Materials & Interfaces*, 2019, 11(27): 23840-23847.
- [67] Dong Z Z, Wang Y D, Wang C L, et al. Cationic peptidopolysaccharide with an intrinsic AIE effect for combating bacteria and multicolor imaging [J]. *Advanced Healthcare Materials*, 2020, 9 (13): e2000419.
- [68] Liu H X, Xiong L H, Kwok R T K, et al. AIE bioconjugates for biomedical applications [J]. *Advanced Optical Materials*, 2020, 8(14): 2000162.
- [69] Sheng Z, Guo B, Hu D, et al. Bright aggregation-induced-emission dots for targeted synergistic NIR-II fluorescence and NIR-I photoacoustic imaging of orthotopic brain tumors [J]. *Advanced Materials*, 2018, 30(29): e1800766.
- [70] Li Y X, Hu D H, Sheng Z H, et al. Self-assembled AIEgen nanoparticles for multiscale NIR-II vascular imaging [J]. *Biomaterials*, 2021, 264: 120365.
- [71] Sheng Z H, Li Y X, Hu D H, et al. Centimeter-deep NIR-II fluorescence imaging with nontoxic AIE probes in nonhuman primates [J]. *Research*, 2020, 2020: 4074593.
- [72] Feng Z, Bai S Y, Qi J, et al. Biologically excretable aggregation-induced emission dots for visualizing through the marmosets intravittally: horizons in future clinical nanomedicine [J]. *Advanced Materials*, 2021, 33(17): e2008123.
- [73] So M K, Xu C J, Loening A M, et al. Self-illuminating quantum dot conjugates for *in vivo* imaging [J]. *Nature Biotechnology*, 2006, 24 (3): 339-343.
- [74] Medintz I L, Uyeda H T, Goldman E R, et al. Quantum dot bioconjugates for imaging, labelling and sensing [J]. *Nature Materials*, 2005, 4(6): 435-446.
- [75] Zhang L J, Xia L, Xie H Y, et al. Quantum dot based biotracking and biodetection [J]. *Analytical Chemistry*, 2019, 91(1): 532-547.
- [76] Hong G S, Robinson J T, Zhang Y J, et al. *In vivo* fluorescence imaging with Ag_2S quantum dots in the second near-infrared region [J]. *Angewandte Chemie*, 2012, 51(39): 9818-9821.
- [77] Li C Y, Cao L M, Zhang Y J, et al. Preoperative detection and intraoperative visualization of brain tumors for more precise surgery: a new dual-modality MRI and NIR nanoprobe [J]. *Small*, 2015, 11(35): 4517-4525.
- [78] Li C Y, Zhang Y J, Chen G C, et al. Engineered multifunctional nanomedicine for simultaneous stereotactic chemotherapy and inhibited osteolysis in an orthotopic model of bone metastasis [J]. *Advanced Materials*, 2017, 29(13): 1605754.
- [79] Li C Y, Chen G C, Zhang Y J, et al. Advanced fluorescence imaging technology in the near-infrared-II window for biomedical applications [J]. *Journal of the American Chemical Society*, 2020, 142 (35):

- 14789-14804.
- [80] Wen Q X, Zhang Y J, Li C Y, et al. NIR-II fluorescent self-assembled peptide nanochain for ultrasensitive detection of peritoneal metastasis [J]. *Angewandte Chemie*, 2019, 58(32): 11001-11006.
- [81] Lian W, Tu D T, Hu P, et al. Broadband excitable NIR-II luminescent nano-bioprobes based on CuInSe₂ quantum dots for the detection of circulating tumor cells [J]. *Nano Today*, 2020, 35: 100943.
- [82] Bouzigues C, Gacoin T, Alexandrou A. Biological applications of rare-earth based nanoparticles [J]. *ACS Nano*, 2011, 5(11): 8488-8505.
- [83] Sun L D, Wang Y F, Yan C H. Paradigms and challenges for bioapplication of rare earth upconversion luminescent nanoparticles: small size and tunable emission/excitation spectra [J]. *Accounts of Chemical Research*, 2014, 47(4): 1001-1009.
- [84] Zhang X, He S Q, Ding B B, et al. Cancer cell membrane-coated rare earth doped nanoparticles for tumor surgery navigation in NIR-II imaging window [J]. *Chemical Engineering Journal*, 2020, 385: 123959.
- [85] Xie Y L, Shen B, Zhou B S, et al. Progress in research on rare-earth upconversion luminescent nanomaterials and bio-sensing [J]. *Chinese Journal of Lasers*, 2020, 47(2): 0207017.
谢荧玲, 沈博, 周兵帅, 等. 稀土上转换发光纳米材料及生物传感研究进展 [J]. 中国激光, 2020, 47(2): 0207017.
- [86] Wang P Y, Fan Y, Lu L F, et al. NIR-II nanoprobes *in-vivo* assembly to improve image-guided surgery for metastatic ovarian cancer [J]. *Nature Communications*, 2018, 9: 2898.
- [87] Li H, Wang X, Li X L, et al. Clearable shortwave-infrared-emitting NaErF₄ nanoparticles for noninvasive dynamic vascular imaging [J]. *Chemistry of Materials*, 2020, 32(8): 3365-3375.
- [88] Yang J Y, He S Q, Hu Z H, et al. *In vivo* multifunctional fluorescence imaging using liposome-coated lanthanide nanoparticles in near-infrared-II/a/II b windows [J]. *Nano Today*, 2021, 38: 101120.
- [89] Welsher K, Liu Z, Sherlock S P, et al. A route to brightly fluorescent carbon nanotubes for near-infrared imaging in mice [J]. *Nature Nanotechnology*, 2009, 4(11): 773-780.
- [90] Hong G S, Diao S, Chang J L, et al. Through-skull fluorescence imaging of the brain in a new near-infrared window [J]. *Nature Photonics*, 2014, 8(9): 723-730.
- [91] Diao S, Blackburn J L, Hong G S, et al. Fluorescence imaging *in vivo* at wavelengths beyond 1500 nm [J]. *Angewandte Chemie International Edition*, 2015, 54(49): 14758-14762.
- [92] Zhou H, Li S S, Zeng X D, et al. Tumor-homing peptide-based NIR-II probes for targeted spontaneous breast tumor imaging [J]. *Chinese Chemical Letters*, 2020, 31(6): 1382-1386.
- [93] Linssen M D, Ter Weele E J, Allersma D P, et al. Roadmap for the development and clinical translation of optical tracers cetuximab-800CW and trastuzumab-800CW [J]. *Journal of Nuclear Medicine: Official Publication, Society of Nuclear Medicine*, 2019, 60(3): 418-423.
- [94] Steinkamp P J, Pranger B K, Li M F, et al. Fluorescence-guided visualization of soft-tissue sarcomas by targeting vascular endothelial growth factor A: a phase 1 single-center clinical trial [J]. *Journal of Nuclear Medicine: Official Publication, Society of Nuclear Medicine*, 2021, 62(3): 342-347.
- [95] Lamberts L E, Koch M, de Jong J S, et al. Tumor-specific uptake of fluorescent bevacizumab-IRDye800CW microdosing in patients with primary breast cancer: a phase I feasibility study [J]. *Clinical Cancer Research*, 2017, 23(11): 2730-2741.

Recent Progress in Near-Infrared-II Fluorescence Imaging Probes for Fluorescence Surgical Navigation

Wei Zuwu, Yang Sen, Wu Ming, Liu Xiaolong*

Mengchao Hepatobiliary Hospital of Fujian Medical University, Fuzhou, Fujian 350025, China

Abstract

Significance Cancer is a major public health challenge that threatens human health and social development. Cancer incidence has exhibited a high growth trend worldwide, where 19.3 million new cases and approximately ten million related deaths were reported in 2020. Surgery is currently the first choice for treating solid tumors. Complete

resection of the tumor is very important for prognosis and long-term survival of patients, whereby the survival rate after complete resection is 2–5 times higher than that after partial resection. However, the global average recurrence rate after tumor resection is still as high as 40%, resulting in 80% mortality in cancer-recurring cases. The main reasons for high postoperative recurrence rate include various key factors, including residual tumor margins caused by incomplete operation, residual micro-metastases or small lesions that are difficult to find during the operation, and micro-metastasis of lymph nodes. In clinical diagnosis before surgery, medical doctors use ultrasound imaging (US), computed X-ray tomography (CT), positron emission tomography (PET), magnetic resonance imaging (MRI), and other imaging methods for accurate tumor localization and morphological confirmation. However, during the operation, doctors can only determine the tumor boundary, residual lesions, and micro-metastatic lesions via limited means of naked-eye observation, palpation, and ultrasound examination. This can easily cause residual surgical margin or missed detection of small lesions during the operation, leading to a high rate of recurrence and metastasis after operation, as well as impacting the prognosis and long-term survival of patients. Thus, there is an urgent need to develop a real-time operation guiding technology without radiation and with high sensitivity, high resolution, and high contrast, which can accurately determine the tumor boundary, display the important duct structure, and detect micro-metastatic lesions during the operation. The fluorescence surgical navigation technology arises at the historic moment.

Progress Fluorescence surgical navigation technology relies on a fluorescence imaging system and fluorescence probe to display focus information more accurately during operation. Presently, the fluorescence surgical navigation probes approved for clinical use include sodium fluorescein, 5-aminolevulinic acid (5-ALA), methylene blue (MB), and indocyanine green (ICG). However, the excitation and emission wavelengths of sodium fluorescein, 5-ALA, and MB locate in the 400–700 nm region. Consequently, the penetration depth is very limited, only tissue surface imaging can be performed, and the signal-to-noise ratio is also very low. Therefore, applying these probes in surgical navigation has been gradually eliminated in the clinic. To achieve deeper tissue penetration depth and conduct more accurate fluorescence imaging and surgical navigation, it is necessary to use near-infrared fluorescence probes with longer excitation and emission wavelengths. Indocyanine green (ICG) is presently the most widely used and thoroughly studied near-infrared fluorescence molecular probe in fluorescence surgical navigation. ICG, which Kodak Laboratory first synthesized in Japan in 1955, can be excited by light at the wavelength of 750–810 nm and emit near-infrared light with the maximum wavelength of 830 nm [Fig. 3(a)]. The near-infrared fluorescence surgical navigation technique based on ICG has been widely used in the field of tumor surgery, and many clinical studies have confirmed its clinical value in the aspects of surgical thoroughness, surgical convenience, recurrence-free survival, and total survival. However, NIR-I fluorescence imaging still has a series of inherent bottlenecks, such as low penetration depth, high background signal, poor signal-to-noise ratio, etc. Recently, with the deepening of NIR-II fluorescence imaging research and the rapid development of nanotechnology, a series of small organic molecules, organic nano-probes and inorganic nano-probes have been developed and used as NIR-II fluorescence molecular probes in the fields of fluorescence imaging and surgical navigation. In 2018, Professor Oliver T. Bruns and colleagues found that the tail band emission of ICG extended to NIR-II, although its emission spectrum reached its peak at NIR-I. In 2020, Tian Jie and colleagues completed a human trial of surgical resection of liver cancer guided by ICG NIR-II fluorescence imaging, and confirmed in clinical practice that this technique can find small and metastatic lesions of liver cancer that other imaging modes cannot detect, and significantly improves the thoroughness and accuracy of surgical resection [Fig. 4(b)–(c)]. Inorganic quantum dots (Ag_2S) show good results in *in vivo* fluorescence imaging of NIR-II region. *In situ* and real-time imaging, high tissue penetration depth (>1.5 cm), high time resolution (~ 30 ms), and high spatial resolution ($\sim 25 \mu\text{m}$) are obtained in *in vivo* level of small animals. Simultaneously, Ag_2S quantum dots can significantly improve the accuracy and thoroughness of surgical resection in NIR-II fluorescence surgical navigation of gliomas [Fig. 8(a)] and breast cancer metastases [Fig. 8(b),(d)]. Additionally, there are several organic and inorganic nanoparticles with excellent performances in NIR-II fluorescence imaging, showing great potential in fluorescence surgical navigation application, such as donor-receptor organic small-molecule fluorescence probes, organic polymer nano-probes, aggregation-induced emission fluorescence probes, and rare earth nano-probes.

Conclusions and Prospects The rapid development of NIR-II fluorescence imaging technology provides new opportunities and means to solve the bottleneck problems in surgical navigation. With the cross-integration of material science, chemistry, and optics, a series of NIR-II fluorescence surgical navigation molecular probes have

been developed. However, these works are still in the stage of basic research and animal experiments. Clinical translation of these probes, which requires combined efforts from enterprises, hospitals, clinicians, and basic researchers, is yet to be promoted. Encouragingly, some preclinical studies have shown good clinical prospects, and laid a foundation for further promoting the translation and application of NIR-II fluorescence surgery navigation. This will provide a strong guarantee for precision surgery in the future.

Key words medical optics; fluorescence surgical navigation; fluorescence probe; near-infrared second window; laparoscopic surgery system; molecular imaging probe